Geometric thermodynamics of strain-induced crystallization in polymers

Sanhita Das [1,2,*] Asif Raza [1,†] and Debasish Roy [1,2,‡]

[1] *Computational Mechanics Laboratory, Department of Civil Engineering, Indian Institute of Science, Bangalore 560012, India*

[2] *Centre of Excellence on Advanced Mechanics of Materials, Indian Institute of Science, Bangalore 560012, India*

(Received 27 December 2021; accepted 6 July 2022; published 25 July 2022)

Going beyond the classical Gaussian approximation of Einstein's fluctuation theory, Ruppeiner gave it a Riemannian geometric structure with an entropic metric. This yielded a fundamental quantity, the Riemannian curvature, which was used to extract information on the nature of interactions between molecules in fluids, ideal gases, and other open systems. In this article, we examine the implications of this curvature in a nonequilibrium thermodynamic system where relaxation is sufficiently slow so as not to invalidate the local equilibrium hypothesis. The nonequilibrium system comprises a rubbery polymer undergoing strain induced crystallization. The curvature is found to impart information on a spurious isochoric energy arising from the conformational stretching of already crystallized segments. This unphysical component perhaps arises as the crystallized manifold is considered Euclidean with the stretch measures defined via the Euclidean metric. The thermodynamic state associated with curvature is the key to determine the isochoric stretch and hence the spurious energy. We determine this stretch and propose a form for the spurious free energy that must be removed from the total energy in order for the correct stresses to be recovered.

DOI: 10.1103/PhysRevE.106.015005

I. INTRODUCTION

Contrary to the notion that thermodynamics describes only macroscopic material behavior, it also affords information on microstates through the fluctuation theory [1]. The Gaussian approximation to the thermodynamic fluctuation theory yields the probability of finding a system in a given thermodynamic state close to equilibrium [1]. However, the Gaussian approximation holds if the volume of the system is very large vis-á-vis fluctuations in the intensive variables. As pointed out by [2], when such conditions are not met, there arise issues of inconsistency and lack of covariance (i.e., coordinate dependence). Depending on the scenario, there is thus a need to go beyond the Gaussian approximation [1,2]. Distributions with characteristics free of these shortcomings are shown to satisfy a diffusion equation involving coefficients, which necessarily satisfy the metric transformation rules of Riemannian geometry. This indicates that the thermodynamic manifold generated by the possible microstates is Riemannian.

Reference [3] presented an approach to introduce a Riemannian structure to the classical fluctuation theory, thereby nontrivially modifying it. It also highlights a new quantity: the thermodynamic Riemannian curvature, which emerges from the Riemannian structure of the thermodynamic manifold. This quantity contains rich information on the underlying fluctuations. Subsequently, [1,4–8] employed this geometrically motivated thermodynamic fluctuation theory to several open thermodynamic systems such as ideal gases, paramagnets, van der Waals gases, and fluids with single or multiple components. In fluids, the curvature is strongly correlated with the nature of interactions with a reversal in sign through critical values.

The implications of the thermodynamic fluctuation theory in polymers have always been of interest to mechanicians [9] especially for semiflexible polymers. For flexible polymers where chains can be microscopically idealized as comprising pin-jointed freely rotating rigid links, we may specifically adopt the affine three-chain network model by [10] which relates the microscopic and macroscopic free energies. In this case, the macroscopic free energy in response to the hyperelastic deformation typically observed in such polymers assumes a neo-Hookean form. The thermodynamic fluctuation theory in such a case predicts a Gaussian probability distribution for the effective average macroscopic stretch. The case is, however, not so simple for semiflexible polymers where the constituting monomers impart bending, extensional, or torsional stiffnesses to the links that were assumed rigid for flexible polymers. Also constraints such as entanglements or cross-links demand the use of nonaffine network models. Moreover, if the macroscopic deformation induces additional inelastic mechanisms such as plasticity, damage, or strain-induced crystallization, additional free energy components due to the formation of defects or appearance of inelastic dissipation need to be considered. The total free energy is then not only a function of the macroscopic or microscopic stretch, but also of other variables, e.g., internal variables, describing the particular inelastic phenomenon. The information afforded by a fluctuation theory on the underlying microstates should shed light on the underlying mechanics. It would also be of interest to see what additional information the scalar curvature described in [1,4–8] provides. If it were to

*sanhitadas@iisc.ac.in
†asifraza@iisc.ac.in
‡royd@iisc.ac.in

show criticality at some particular thermodynamic state, then the natural question is what we could say about the process itself. This might offer insights into whether we might put this criticality to some advantage. Finally, Ruppeiner limited his analysis to purely equilibrium systems. The important issue of extending this useful construct to systems undergoing nonequilibrium changes also remains unresolved at this time.

In an attempt to partially answer some of these questions on polymer inelasticity, we explore the implications of introducing a Riemannian structure to the fluctuation theory in line with [3] and others. Specifically, we rely on the emerging curvature to reveal the microscale information of a thermodynamic system describing strain induced crystallization (SIC) in a rubber specimen. SIC is a nonequilibrium phenomenon in which regions of a rubber sample undergo crystallization when stretched. At the molecular level, polymer chain segments in these regions orient themselves in the direction of locally developed tension and weak intermolecular bonds are formed in between adjacent straightened segments, establishing a relatively long range order in the region. On removal of deformation or in the event of a reversal of the local tensile stress, the segments fall into a state of disorder and crystallization is lost.

Strain-induced crystallization is intrinsically a nonequilibrium phenomenon, but it is still possible to exploit Ruppeiner's approach if the local equilibrium hypothesis holds. We recall that this hypothesis is posited on two conditions. The first one is that an RVE (the smallest volume of material whose effective behavior is representative of the material as a whole) is sufficiently large so that the relative fluctuations of the extensive thermodynamic variables can be ignored. In contrast, the second one requires the RVE to be small enough to ensure local homogeneity of the macroscopic (continuum) response. Since smaller spatial scales typically have fluctuations with higher frequency, the choice of the RVE size is intricately related to the temporal fluctuations of quantities of relevance at the micro- and macroscales.

In this context, we note that the timescale typically associated with the crystallization of strained polymers (rubber) is orders larger than that for atomistic vibrations, even as it is smaller than the timescale of structural relaxation in a polymeric glass. References [11,12] observe that the timescale associated with crystallization is 4 s. The total timescale includes the timescale for nucleation as well as that for the growth of crystallites. Furthermore, [13] predicts the total timescale in vulcanized natural crepe rubber to range from 10 to 100 s depending on the ambient temperature. According to that work, the growth phase in crystallization is strongly dependent on the mobility of the chains and therefore on temperature and strain rate. Temperature and strain rate therefore have a strong influence on the overall rate of crystallization. Indeed, it is only for very low temperatures (lower than $-25\,^{\circ}$C) and large strain rates that the rate of crystallization is high, which translates to a low characteristic timescale. In the range of temperatures considered in this article, the characteristic timescale is orders above that for atomistic vibrations. Also, crystallized segments constitute mesoscale structures, which are larger than molecular dimensions and allow local thermodynamic states to be defined. For instance, the size of a single crystallite is of the order of 10 nm [14] and a single RVE contains several such structures. Thus, if a process has a timescale appropriate for the local equilibrium hypothesis and can be described using a number of metastable equilibrium states characterised by local, instantaneously equilibrating state variables or internal variables, Ruppeiner's approach should be applicable as all axioms of equilibrium thermodynamics remain valid (see [15–18]).

Moreover, the same local equilibrium hypothesis has been the basis for several constitutive theories for polymers in general and for strain-induced crystallization in particular [19–24].

We further assume that crystallization takes place isotropically so every chain in the RVE [10] undergoing SIC and macroscopically represented by a material point has the same "degree of crystallization" (defined as the fraction of chain segments already crystallized). The free energy of such a partially crystallized specimen is derived along the lines of [19,23,24].

We then define the thermodynamic manifold for the system in local equilibrium, where the coordinates are given by the state variables that fluctuate. Then the metric, the affine connection, and the invariant scalar curvature are derived. The variation in scalar curvature over the manifold is analyzed for any critical points and the physical significance of these points is assessed for their relevance to the total free energy density and the strain energy density. Finally, we investigate the possible exploitation of this kinematically relevant information to redefine the free energy density. The critical points, as it turns out, correspond to states with unphysical conformational stretches. We infer that, by not accounting for the non-Euclidean geometric aspects imparted by crystallization, earlier constitutive theories ([23,24]) yield stretch measures incapable of eliminating components due to the already crystallized segments. We identify these stretches and thus propose a form for the spurious energy to be eliminated from the total free energy.

The rest of the article is organized as follows. We provide definitions and some background information on the Riemannian thermodynamic manifold and its metric and curvature in Sec. II. This is followed in Sec. III by the definition of the free energy of a polymer undergoing SIC. The free energy is then used to determine the metric and the curvature in Sec. IV. Analytical computation of geometric quantities in a seven- or eight-dimensional manifold is immensely complicated. Hence, to simplify calculations, we consider two cases of deformation: uniaxial tension and simple shear. Coordinates corresponding to the components of the right Cauchy-Green tensor may thus be expressed as functions of fewer coordinates representing the uniaxial tensile stretch in an incompressible or a compressible material or the magnitude of shear strain in an incompressible material. This section also describes the physical implication of curvature through a comparison of its variation over the manifold with those of free energy and strain energy densities. Section V defines the spurious isochoric free energy component as a function of the strain determined in the earlier section. The total free energy is also redefined after removal of this spurious energy. The article is finally concluded in Sec. VI.

II. GEOMETRY OF RIEMANNIAN THERMODYNAMIC MANIFOLDS

The basic geometry is based on two fundamental axioms of equilibrium thermodynamics [3].

(i) In any thermodynamic system with a fixed scale, there exist equilibrium states which can be represented by points on a higher-dimensional manifold which is differentiable everywhere, considering no phase transitions and critical points. The coordinates associated with the manifold are the independent state variables describing the equilibrium states.

(ii) On the manifold, there exists a positive definite Riemannian metric **g**, which is determined (at any point on the manifold) by the condition that its components in a particular coordinate system are the second moments of fluctuations of the thermodynamic states.

Let us consider a thermodynamic manifold with points denoting the entropy density η of a system. Let the manifold be parametrized by a set of thermodynamic states $x = (x_1, x_2, \ldots, x_n)$. If we choose to adopt the standard entropy representation of a thermodynamic system in line with [25], then x_1 is the internal energy density ϵ of the system and the rest of the variables are mechanical parameters expressed as standard densities. For such a parametrization, Ref. [2] states that a metric tensor **g** satisfying the requirements of covariance and consistency must have its components as follows:

$$g_{ij} = -\frac{1}{k_B}\frac{\partial^2 \eta}{\partial x_i \partial x_j}. \tag{1}$$

The positive definite quadratic form defining the distance between two states on the entropic manifold is given by

$$(\Delta l)^2 = \sum_{i,j=0}^{n} g_{ij}\Delta x_i \Delta x_j. \tag{2}$$

For any other parametrization, the quadratic form must be expressed in transformed coordinates, and that should accordingly yield the components of the metric in the transformed space. For instance, if we wish to transform from $x = (\epsilon, x_2, \ldots, x_n)$ to $x = (T, x_2, \ldots, x_n)$, where T is the absolute temperature, then in line with [2] the line element is

$$(\Delta l)^2 = \frac{1}{k_B T}\left(\frac{\partial \eta}{\partial T}\right)(\Delta T)^2 + \frac{1}{k_B T}\sum_{i,j=1}^{2}\left(\frac{\partial f_i}{\partial x_j}\right)\Delta x_i \Delta x_j. \tag{3}$$

Here $f_i = (\frac{\partial \psi}{\partial x_i})_T$, where ψ is the Helmholtz free energy

Using $\eta = -\frac{\partial \Psi}{\partial T}$ and the expression for f_i, the quadratic form can be expressed as a function of the free energy [8],

$$(\Delta l)^2 = -\frac{1}{k_B T}\left(\frac{\partial^2 \Psi}{\partial T^2}\right)(\Delta T)^2 + \frac{1}{k_B T}\sum_{i,j=1}^{2}\left(\frac{\partial^2 \Psi}{\partial x_i \partial x_j}\right)\Delta x_i \Delta x_j. \tag{4}$$

This can be used to find the metric components in the new space. If we consider a three-dimensional thermodynamic manifold parametrized by $x = (T, x_1, x_2)$, the metric assumes the form

$$g_{ij} = \frac{1}{k_B T}\begin{bmatrix} -\frac{\partial^2 \Psi}{\partial T^2} & 0 & 0 \\ 0 & \frac{\partial^2 \Psi}{\partial x_1^2} & \frac{\partial^2 \Psi}{\partial x_1 \partial x_2} \\ 0 & \frac{\partial^2 \Psi}{\partial x_2 \partial x_1} & \frac{\partial^2 \Psi}{\partial x_2^2} \end{bmatrix}. \tag{5}$$

The Christoffel symbols $\mathbf{\Gamma}^k_{ij}$ associated with the affine connection are given by

$$\mathbf{\Gamma}^k_{ij} = g^{km}\frac{1}{2}\left[\frac{\partial g_{im}}{\partial x^j} + \frac{\partial g_{jm}}{\partial x^i} - \frac{\partial g_{ij}}{\partial x^m}\right]. \tag{6}$$

These are then used to calculate the Riemannian curvature tensor $\tilde{\mathbf{R}}$ whose components may be expressed as

$$\tilde{R}^l_{ijk} = \frac{\partial}{\partial X^i}\mathbf{\Gamma}^l_{jk} - \frac{\partial}{\partial X^j}\mathbf{\Gamma}^l_{ik} + \mathbf{\Gamma}^l_{im}\mathbf{\Gamma}^m_{jk} - \mathbf{\Gamma}^l_{jm}\mathbf{\Gamma}^m_{ik}. \tag{7}$$

Upon contraction, we have the symmetric Ricci tensor $\hat{\mathbf{R}}$,

$$\hat{R}_{ij} = \tilde{R}^k_{ikj}, \tag{8}$$

as well as the Ricci scalar curvature R,

$$R = g^{jj}\tilde{R}^k_{ikj}, \tag{9}$$

where g^{jj} is the inverse (or the contravariant form) of the metric g_{ij}.

III. FREE ENERGY OF A PARTIALLY CRYSTALLIZED POLYMER

On a continuum level, let $\varphi : \mathbf{X} \mapsto \mathbf{x}$ be a diffeomorphism that maps material points $\mathbf{X} \in \mathcal{B}$ of the reference configuration $\mathcal{B} \subset \mathbb{R}^3$ to points $\mathbf{x} = \varphi(\mathbf{X}; \mathbf{t}) \in \mathcal{S}$ of the current configuration $\mathcal{S} \subset \mathbb{R}^3$. Define the deformation gradient as $\mathbf{F} := \nabla\varphi(\mathbf{X}; \mathbf{t})$ with Jacobian $J := \det \mathbf{F} > 0$. The polymer is considered slightly compressible; therefore $\mathbf{F}$ is decomposed into volumetric and isochoric parts denoted respectively by $\mathbf{F}_{\text{vol}}$ and $\bar{\mathbf{F}}$ [23]:

$$\mathbf{F} = \mathbf{F}_{\text{vol}}\bar{\mathbf{F}}, \quad \text{where} \quad \mathbf{F}_{\text{vol}} = J^{1/3}\mathbf{I} \text{ and } \bar{\mathbf{F}} = J^{-1/3}\mathbf{F}. \tag{10}$$

If $\mathbf{C}$ denotes the right Cauchy-Green tensor, its isochoric component is given by

$$\bar{\mathbf{C}} = J^{-2/3}\mathbf{C}. \tag{11}$$

The total free energy density is considered as a function of $\mathbf{C}$, the ambient temperature T, and the internal variable Ω, which is a macroscopic measure of the degree of crystallinity in the material:

$$\Psi = \Psi(\mathbf{C}, \Omega, T). \tag{12}$$

In particular, Ω is the ratio of the volume of crystallized polymeric segments to the total volume of the RVE. Thus, if N_T is the total number of polymeric segments in the RVE, the total number of crystallized segments in the RVE is ΩN_T. The total free energy density may be written as the sum of a strain energy consisting of volumetric and isochoric parts, a crystalline free energy, and the energy due to surrounding heat interactions:

$$\Psi = \Psi_{\text{strain}}(\bar{\mathbf{C}}, \Omega, T) + \Psi_{\text{cr}}(\Omega, T) + \Psi_{\text{surr}}(T). \tag{13}$$

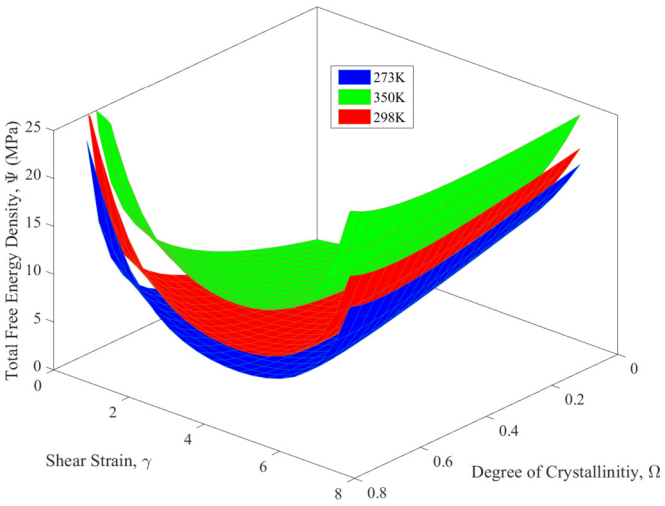

FIG. 1. Free energy surfaces for an incompressible material under simple shear and different temperatures T.

As noted, the strain energy Ψ_{strain} comprises a deviatoric component and a volumetric component:

$$\Psi_{\text{strain}} = \Psi_{\text{vol}}(J) + \Psi_{\text{dev}}(\bar{\mathbf{C}}, \Omega, T), \tag{14}$$

where the volumetric free energy Ψ_{vol} is given by

$$\Psi_{\text{vol}} = \tfrac{1}{2}B(J-1)^2, \tag{15}$$

and B is the bulk modulus. The isochoric strain energy component is the average of the strain energy of all the chains in the RVE. Mesocopically speaking, the chains might have different stretches and orientations in response to the deformation $\mathbf{C}$. Ideally, a cubic network of eight chains with orientations along the diagonals and the sides of the cube is used to compute an average stretch λ_a, which is assigned to every chain in the RVE. If n is the number of the equivalent chains per unit volume of the RVE with stretch λ_a, the total isochoric strain energy density Ψ_{dev} may be related to the strain energy Ψ in each equivalent chain by the following relation:

$$\Psi_{\text{dev}}(\mathbf{C}, \Omega, T) = n\Psi(\lambda_a, \Omega, T). \tag{16}$$

The average stretch λ_a of the equivalent chain is given by

$$\lambda_a = \sqrt{I_1/3} \quad \text{where} \quad I_1 = \text{tr}[\bar{\mathbf{C}}]. \tag{17}$$

The strain energy Ψ in each equivalent chain is given by

$$\Psi = k_B T N(1-\Omega)\left[\frac{3}{2}\left(\frac{\lambda_a}{\sqrt{N}}\right)^2 + \frac{9}{20}\left(\frac{\lambda_a}{\sqrt{N}}\right)^4 + \frac{99}{350}\left(\frac{\lambda_a}{\sqrt{N}}\right)^6\right], \tag{18}$$

where N is the number of segments in each equivalent chain. This particular form is derived from the entropy generated due to segmental conformations in the chain [26]. It is important to note that λ_a in the above expression is the stretch in an uncrystallized chain and needs be modified to include the effects of crystallization. If the chain is partially crystallized, only the segments in the uncrystallized zone are free to entropically stretch or compress in response to deformation. In accordance with [23,24], we introduce a modified total stretch Λ_a in a partially crystallized equivalent chain as $\Lambda_a = \frac{\lambda_a/\sqrt{N}-\Omega}{1-\Omega}$. Considering the modified stretch Λ_a and the relation in Eq. (16), the isochoric strain energy assumes the form

$$\Psi_{\text{dev}} = k_B T N n(1-\Omega)\left(\frac{3}{2}\Lambda_a^2 + \frac{9}{20}\Lambda_a^4 + \frac{99}{350}\Lambda_a^6\right). \tag{19}$$

Now we focus on the remaining components of the free energy density. The crystalline free energy is directly adopted from Refs. [23,24,27]:

$$\Psi_{\text{cr}} = -nc\left(1-\frac{T}{T_m}\right)\Omega - n\xi\left[\frac{\Omega}{\Omega_{\max}} + \ln\left(1-\frac{\Omega}{\Omega_{\max}}\right)\right]. \tag{20}$$

The first term on the right-hand side above is the enthalpy of fusion of crystallized segments (see [19]), where c is the heat of fusion per unit segment and T_m is the melting point of the segments. The second term is a penalty term that prevents the crystallization from growing unbounded, i.e., beyond $\Omega_{\max}$. The remaining component, i.e., the surrounding energy, is taken from [28]:

$$\Psi_{\text{surr}} = c_V\left(T - T_0 - T\ln\frac{T}{T_0}\right). \tag{21}$$

c_V is the volumetric heat capacity and T_0 a reference temperature. c_V in rubbers may be considered temperature independent [28–30]. Moreover since the ambient temperatures used in the numerical experiments are above the glass transition temperature of the material, such an assumption does make sense. The total free energy density therefore assumes the following form:

$$\Psi = \frac{1}{2}B(J-1)^2 + k_B T n N(1-\Omega)\left(\frac{3}{2}\Lambda_a^2 + \frac{9}{20}\Lambda_a^4 + \frac{99}{350}\Lambda_a^6\right) - nc\left(1-\frac{T}{T_m}\right)\Omega - n\xi\left[\frac{\Omega}{\Omega_{\max}} + \ln\left(1-\frac{\Omega}{\Omega_{\max}}\right)\right] + c_V\left(T - T_0 - T\ln\frac{T}{T_0}\right). \tag{22}$$

The constitutive equation for the second Piola-Kirchhoff stress is given as

$$\mathbf{S} = 2\frac{\partial\Psi}{\partial\mathbf{C}} = \frac{B}{2}(J-1)J\mathbf{C}^{-1} + \frac{k_B T n\sqrt{N}}{3\lambda_a}J^{-2/3}(1-\Omega)\left(3\Lambda_a + \frac{9}{5}\Lambda_a^3 + \frac{594}{350}\Lambda_a^5\right)\left(\mathbf{I} - \frac{\text{tr}[\mathbf{C}]\mathbf{C}^{-1}}{3}\right). \tag{23}$$

The Cauchy stress is related to $\mathbf{S}$ by

$$\sigma = \frac{\mathbf{F}\mathbf{S}\mathbf{F}^T}{J}. \tag{24}$$

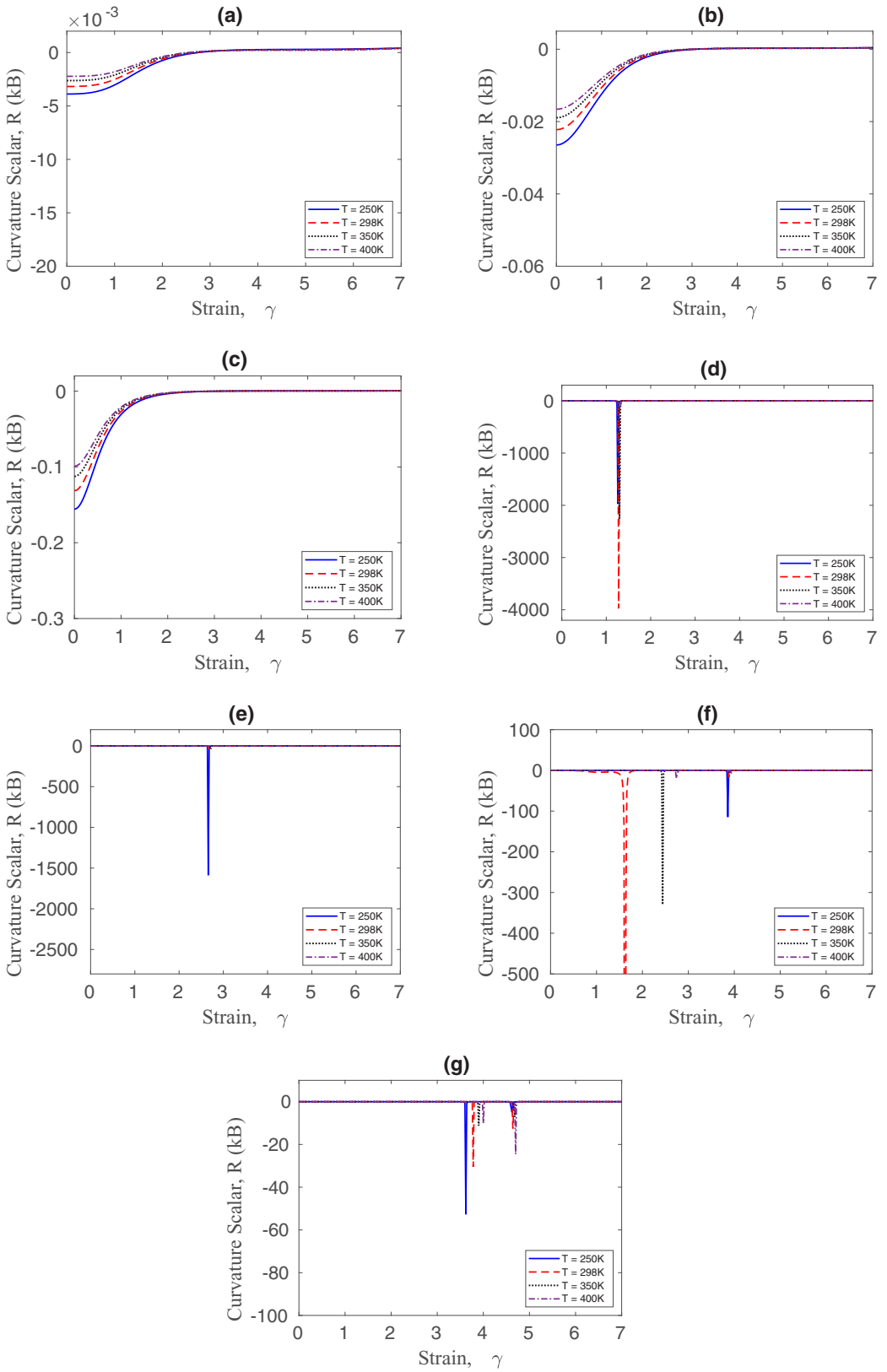

FIG. 2. Plots of scalar curvature R with shear γ at varying temperatures, for crystallization ratios (a) $\Omega = 0$, (b) $\Omega = 0.15$, (c) $\Omega = 0.20$, (d) $\Omega = 0.30$, (e) $\Omega = 0.45$, (f) $\Omega = 0.60$, (g) $\Omega = 0.70$.

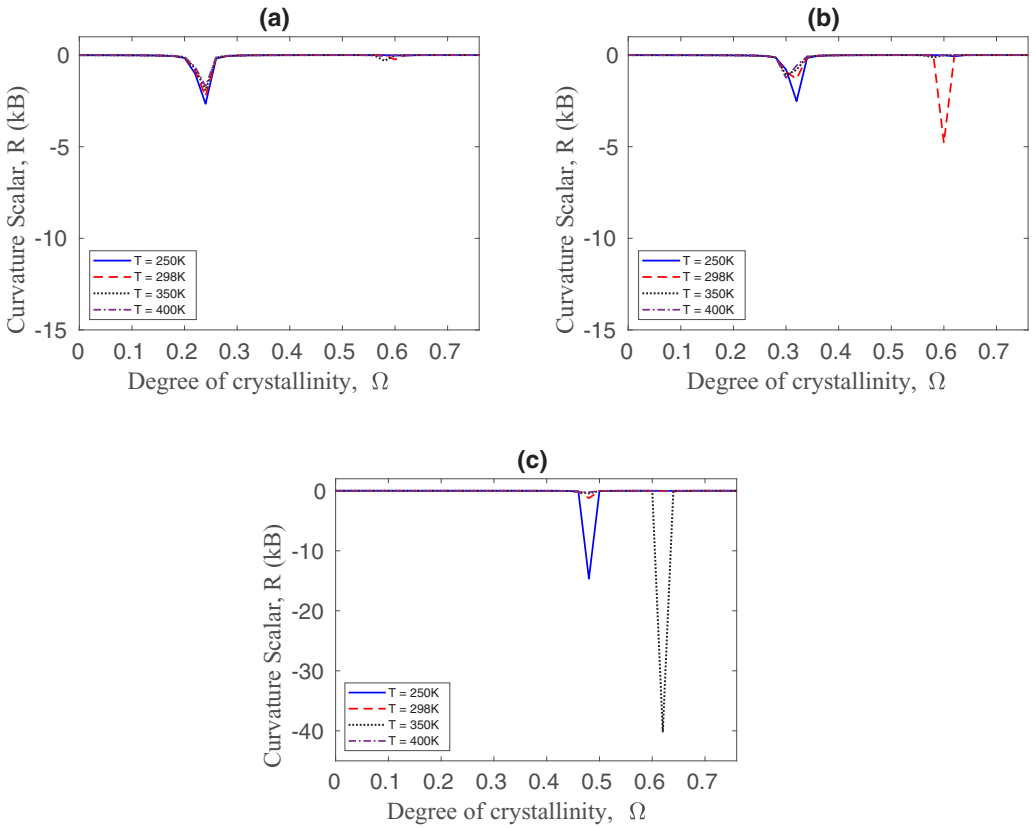

FIG. 3. Plots of scalar curvature R with degree of crystallinity Ω at varying temperatures, for shear strains (a) $\gamma = 0$, (b) $\gamma = 1.4$, (c) $\gamma = 2.9$.

IV. THERMODYNAMIC GEOMETRY OF CRYSTALLIZED POLYMER

Let us consider the temporally fluctuating thermodynamic state $(\mathbf{C}, \Omega, T)$ of the deformed, crystallized polymer. It is important to note that the timescale associated with the fluctuations is orders larger than that associated with crystallization. This enables us to invoke the principle of local equilibrium. The thermodynamic manifold is eight dimensional with coordinates $(C_{11}, C_{12}, C_{13}, C_{22}, C_{23}, C_{33}, \Omega, T)$. The metric and curvature of the system given by Eqs. (5) and (9) may be expressed in the above coordinates.

An attempt to consider fluctuations in all the eight quantities faces the difficulty that the metric and curvature tensors are prohibitively complex, both to compute and to interpret. This necessitates a reduction in the dimension of the thermodynamic phase space. Thus we analyze the system for three specific states of deformation: simple shear, uniaxial tension with material incompressibility. and uniaxial tension allowing for a compressible material. The values for the following material parameters appearing in Eqs. (23) have been adopted from [23] for sulfur cured natural rubber: $N = 18.5$, $n = 8.99 \times 10^{25}\,\mathrm{m}^{-3}$, $c_v = 1.8 \times 10^3\ \mathrm{Nm}^{-2}\,\mathrm{K}^{-1}$, $T_0 = 273$ K, $\Omega_{\max} = 0.78$, $c = 3.5409 \times 10^{-19}$ N m, and $\xi = 1.11 \times 10^{-20}$ N m. $B = 3.576 \times 10^7$ Pa is the value obtained considering the Poisson's ratio to be 0.45. The value of $T_m = 245$ K has been taken from [31].

A. Simple shear deformation in a hyperelastic solid

If γ denotes the shear strain, the deformation gradient for the case of simple shear is given by

$$\mathbf{F} = \begin{bmatrix} 1 & \gamma & 0 \\ 0 & 1 & 0 \\ 0 & 0 & 1 \end{bmatrix} \tag{25}$$

The only nonzero components of the right Cauchy-Green tensor are $C_{11} = C_{33} = 1$, $C_{22} = 1 + \gamma^2$, and $C_{12} = C_{21} = \gamma$. The reduced thermodynamic phase space thus may be represented with just two coordinates, γ and Ω. The average stretch λ_a as obtained from Eq. (17) is $\sqrt{\frac{3+\gamma^2}{3}}$. Using these expressions, we obtain the total free energy from Eq. (22) as a function of γ, Ω, and T. The surfaces generated by the free energy expression for different temperatures are shown in Fig. 1. Using the free energy, the metric and the curvature can be determined. The metric $\mathbf{g}$ in each case is scaled by k_B so as to ensure an accurate inversion of matrices by the software *Mathematica* [32]. The resulting curvature is therefore expressed in k_B units.

To maintain expositional brevity, we avoid writing out the explicit expressions for these quantities.

The scalar curvature R defines a hypersurface in $\mathbb{R}^4$ which is difficult to visualize and interpret. To simplify the analysis, we generate two sets of plots. The first set comprises of plots of R vs γ at various Ω's. Each plot contains curves generated at various ambient temperatures T. In the second

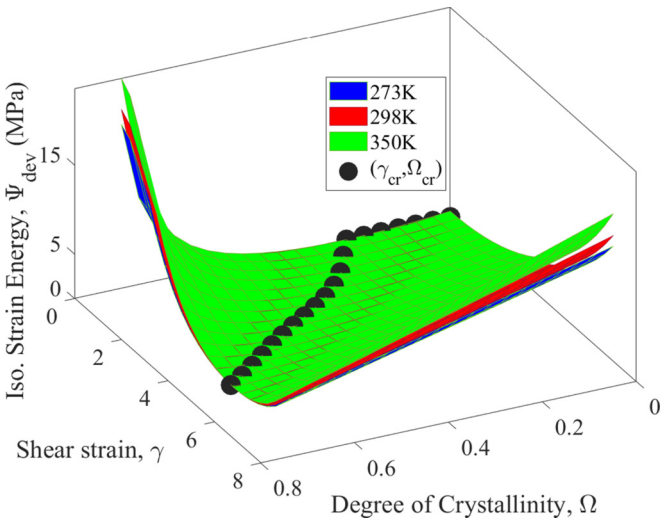

FIG. 4. Strain energy surfaces for different temperatures T.

set, there are plots of R vs Ω for certain critical values of γ, which are determined from the first set of plots. Temperature variation is captured in this set as well. The first set of plots are shown in Fig. 2. Curves corresponding to $\Omega = 0$, 0.15, and 0.2 monotonically increase from an initial curvature till they reach a steady state, whereas for $\Omega > 0.2$ sharp negative peaks are observed breaking the monotonicity. Even though some of these plots have multiple peaks, we can single out a characteristic peak in each of these plots, the strain corresponding to which is independent of temperature. The existence of such a consistent break in the monotonicity hints at some underlying criticality and perhaps a change of response beyond a certain thermodynamic state. Let the critical shear strain values be denoted γ_{cr} corresponding to the chosen Ω.

Across the plots, a temperature invariant peak is observed for all Ω values greater than 0.2. In the second set of plots shown in Fig. 3, the curvature is plotted against Ω. These plots are generated for certain values of γ. To assess the consistency between plots in Figs. 2 and 3, we choose some γ_{cr} as values of γ. As expected, we observe negative peaks at certain Ω values for each γ chosen, which we denote as Ω_{cr}. The Ω_{cr} values obtained for $\gamma = 1.4$ and $\gamma = 2.9$ are the same Ω's at which Figs. 2(d) and 2(e) respectively were plotted. From Fig. 3, specifically the plot corresponding to $\gamma = 0$, we obtain Ω_{cr} to be 0.23, which is nothing but $\frac{1}{\sqrt{N}}$. This confirms that, for all $\Omega_{cr} < \frac{1}{\sqrt{N}}$, γ_{cr} is always 0.

Combining our observations from Figs. 2 and 3, we conclude that some change in physical response occurs at states corresponding to (Ω_{cr}, γ_{cr}), and the values of these states may be obtained graphically. We determine their values to be (0,0), (0,0.15), (0,0.2), (1.4,0.3), (2.7,0.45), (3.9,0.6), (4.7,0.7).

Towards understanding the physical significance of the critical states, we analyze the variation in free energy in the neighbourhood of these states. From Eqs. (5), (6), (7), and (9), we may infer that the only components of free energy contributing to the curvature would be those involving a strong coupling among the thermodynamic states. Hence it suffices

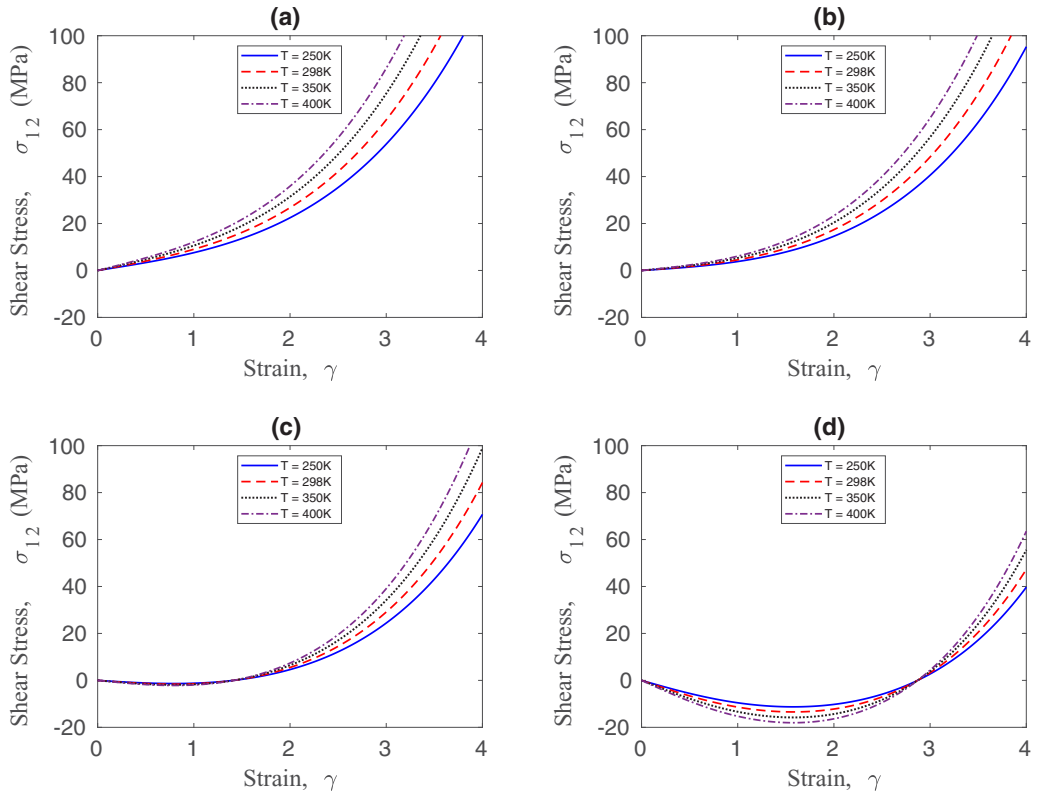

FIG. 5. Plots of σ_{12} with shear strain γ at varying temperatures, for crystallization ratios (a) $\Omega = 0$, (b) $\Omega = 0.15$, (c) $\Omega = 0.30$, (d) $\Omega = 0.45$.

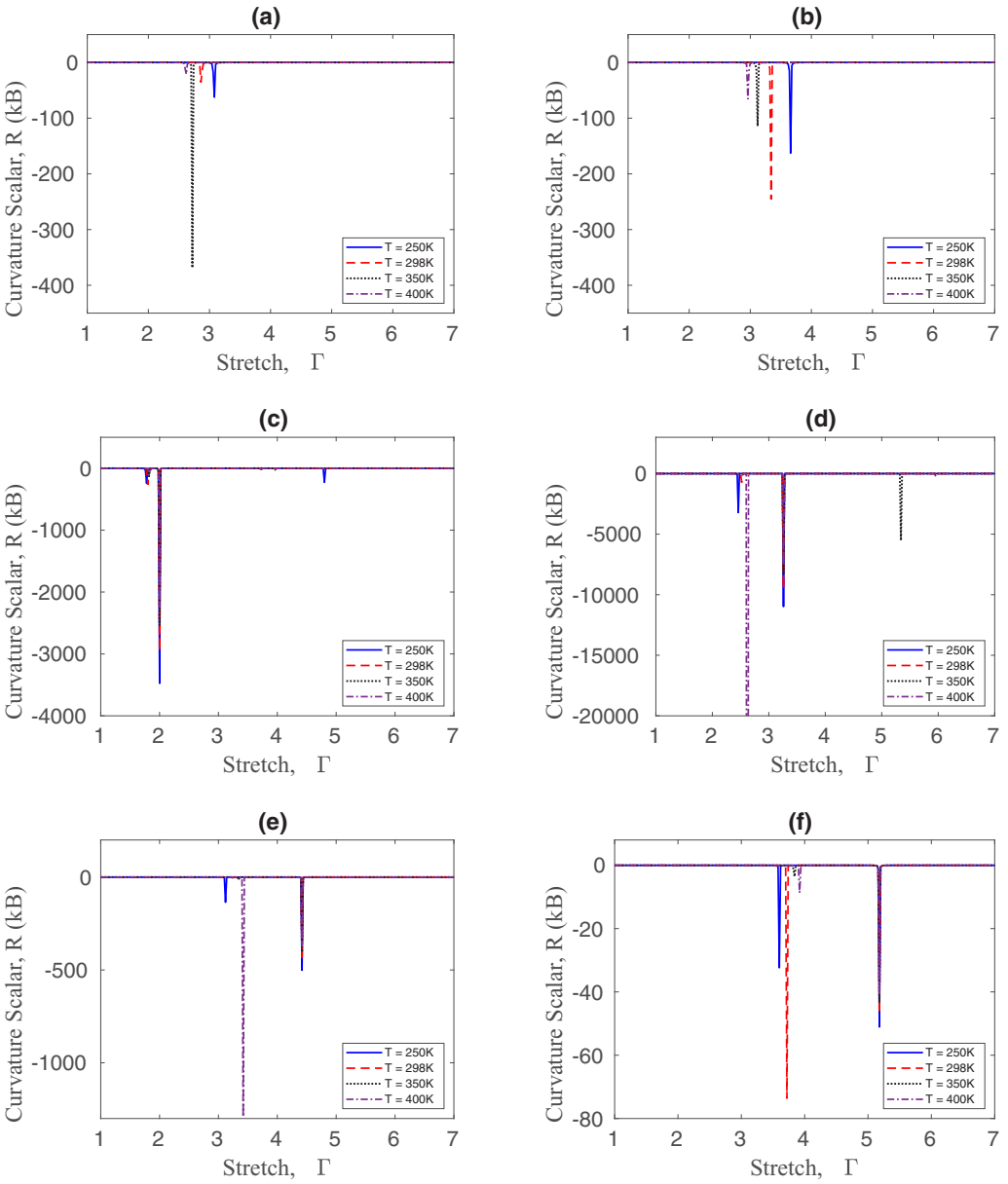

FIG. 6. Plots of scalar curvature R with stretch Γ at varying temperatures, for crystallization ratios (a) $\Omega = 0$, (b) $\Omega = 0.15$, (c) $\Omega = 0.30$, (d) $\Omega = 0.45$, (e) $\Omega = 0.60$, (f) $\Omega = 0.70$.

to analyze the variation of Ψ_{strain} across the thermodynamic space. From Fig. 4, we observe that at $(\gamma_{\text{cr}}, \Omega_{\text{cr}})$, denoted by the black circular markers, this component reduces to zero. The total free energy, however, remains nonzero [see Fig. 1 as well as Eq. (1)] due to the other components Ψ_{cr} and Ψ_{surr} given by Eqs. (20) and (21) respectively.

Upon analyzing the graph and the expression for Ψ_{strain}, all the pairs of $(\gamma_{\text{cr}}, \Omega_{\text{cr}})$ satisfy

$$(\Omega_{\text{cr}}\sqrt{N} - \lambda_{acr})H\left(\Omega_{\text{cr}} - \frac{1}{\sqrt{N}}\right) + (1 - \lambda_{acr})H\left(\frac{1}{\sqrt{N}} - \Omega_{\text{cr}}\right) = 0, \tag{26}$$

where $\lambda_{acr} = \sqrt{\frac{3+\gamma_{\text{cr}}^2}{3}}$.

Let us not limit the set $\{(\gamma_{\text{cr}}, \Omega_{\text{cr}})\}$ to just the pairs obtained graphically, but to any pair satisfying the condition above. Physically, at this state, the applied shear strain γ and the degree of crystallization Ω are such that the effective strain from the conformational changes in the uncrystallized links is 0 and no elastic stress is generated. Also, γ_{cr} may be considered as the internal strain generated solely due to the crystallized segments. A shear strain can only give rise to any elastic conformational stress if it is greater than γ_{cr} for a given Ω_{cr}. However, for any $\gamma < \gamma_{\text{cr}}$, the presence of a finite strain energy is unphysical. Here, the only components contributing to the total free energy should be Ψ_{cr} and Ψ_{surr}. Hence the total free energy should be reduced by a spurious conformational strain energy generated by $\gamma < \gamma_{\text{cr}}$ for a given Ω_{cr}.

That the critical state is a stress-free state is corroborated by the shear stress-strain plots shown in Fig. 5.

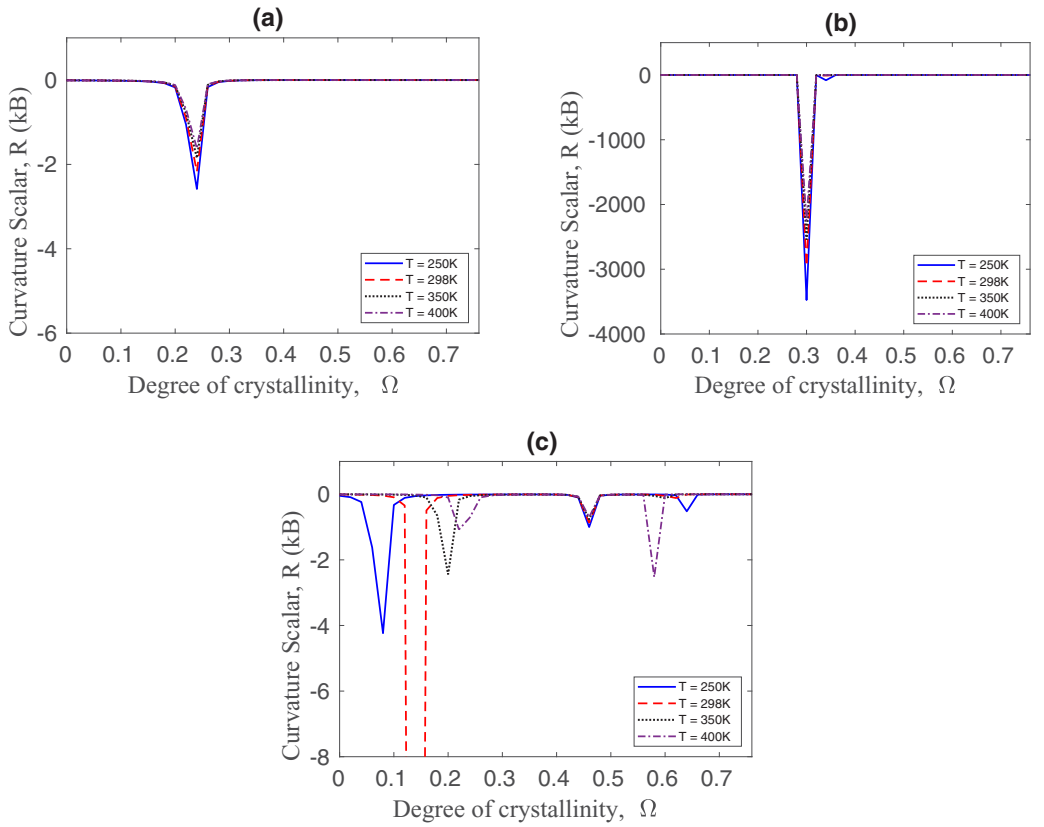

FIG. 7. Plots of scalar curvature R with degree of crystallinity Ω at varying temperatures, for stretch values (a) $\Gamma = 1$, (b) $\Gamma = 2$, (c) $\Gamma = 3.3$.

To investigate the influence of loading condition on the critical state, we study curvature plots in the case of uniaxial tension on an incompressible, hyperelastic solid and under a general strain state that involves slight compression.

B. Uniaxial tension in an incompressible hyperelastic solid

If the tensile stretch is Γ, the deformation gradient assumes the form

$$\mathbf{F} = \begin{bmatrix} \Gamma & 0 & 0 \\ 0 & \Gamma^{-1/2} & 0 \\ 0 & 0 & \Gamma^{-1/2} \end{bmatrix}. \tag{27}$$

The eight-dimensional space is reduced to a three-dimensional manifold by the following relations among the components of the right Cauchy-Green tensor and the tensile stretch: $\Gamma - C_{11} = \Gamma^2$, $C_{22} = C_{33} = \Gamma^{-1}$, the other components of the tensor being 0. The thermodynamic states or the coordinates of the manifold are therefore (Γ, Ω, T).

The scalar curvature is plotted against Γ for various values of Ω and T in Fig. 6.

Unlike the case of simple shear, we observe multiple negative peaks in each plot of Fig. 6, which shows the variation of scalar curvature R with tensile stretch Γ for some chosen Ω values. Considering each plot, out of all the Γ values at which the multiple peaks occur, we identify a single Γ at which a peak is present for all temperatures. Thus this Γ is a temperature independent state at which the curvature consistently displays criticality for a given Ω. This is denoted as Γ_{cr}. The same can be said about the plots in Fig. 7, which shows the variation of scalar curvature R with Ω for selected Γ values, and there are temperature independent Ω's for all the Γ values considered, which we denote as Ω_{cr}.

Thus using the above plots, we can again determine pairs of $(\Gamma_{cr}, \Omega_{cr})$. The pairs thus graphically obtained are (1,0), (1,0.15), (1,0.22), (2,0.3), (3.26,0.45), (4.4,0.6), (5.2,0.7). Γ_{cr}

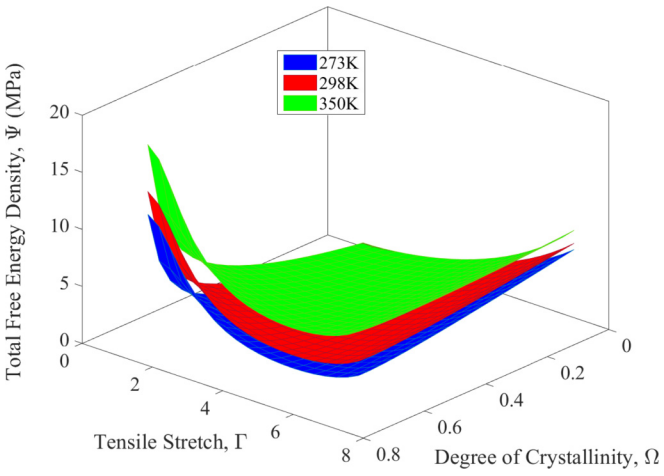

FIG. 8. Free energy surfaces for different temperatures T under uniaxial tension in an incompressible material.

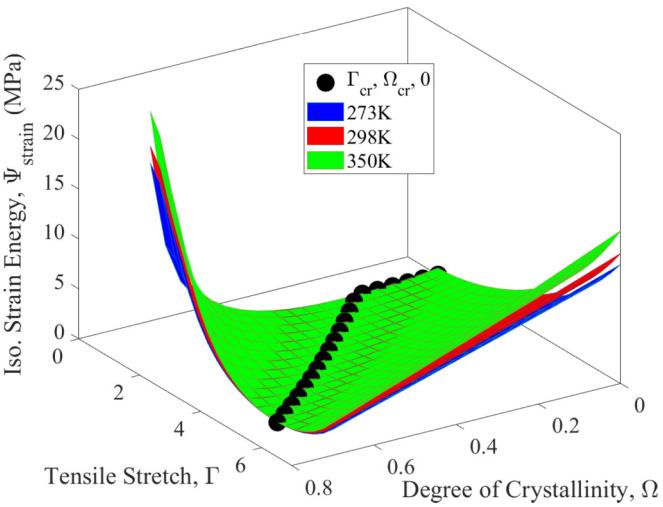

FIG. 9. Strain energy surfaces for different temperatures T for uniaxial tension in an incompressible hyperelastic material.

for $\Omega < \frac{1}{N}$ is again 1. The critical points satisfy condition (26) as well. Also, the strain energy component in the free energy reduces to zero, as is evident in Figs. 8 and 9. Hence we conclude that, even for isochoric uniaxial tension, the critical state retains the same meaning as that in simple shear and that the infeasibility of any state ($\Gamma < \Gamma_{cr}$) for a given Ω_{cr} calls for the consideration of a spurious conformational energy and hence a subsequent reduction in the total free energy.

C. Nonisochoric deformation in a hyperelastic solid

For the previous cases, the volumetric component of free energy and the associated stress were absent either due to the applied deformation being isochoric (in simple shear) or a combination of conditions on the material response and the deformation (uniaxial tension in an incompressible solid). In both of them the critical pairs could be as well identified from the stress plots (Figs. 5 and 10) as the stress at those states reduces to zero.

We now consider a case where the volumetric component contributes to the total free energy and stress, and investigate the information imparted by the scalar curvature. So, this case corresponds to nonisochoric deformation in a compressible solid. Let the deformation gradient be given by

$$\mathbf{F} = \begin{bmatrix} 1+\gamma_n & 0 & 0 \\ 0 & 1 & 0 \\ 0 & 0 & 1 \end{bmatrix}. \tag{28}$$

The eight-dimensional space is reduced to a three-dimensional manifold, similarly to the earlier cases, and the components of the right Cauchy-Green tensor are related to strain γ_n through $C_{11} = (1+\gamma_n)^2$, $C_{22} = C_{33} = 1$. The other components of the tensor are 0. Similar to the isochoric cases, we determine the variation of scalar curvature across the phase space through the plots in Figs. 11 and 12. Also, we obtain the free energy and strain energy surfaces at different temperatures in Figs. 13 and 14, respectively.

In the plots of Fig. 11, nonzero curvature peaks are observed only in the vicinity of or at $\gamma_n = 0$ for all Ω values. The

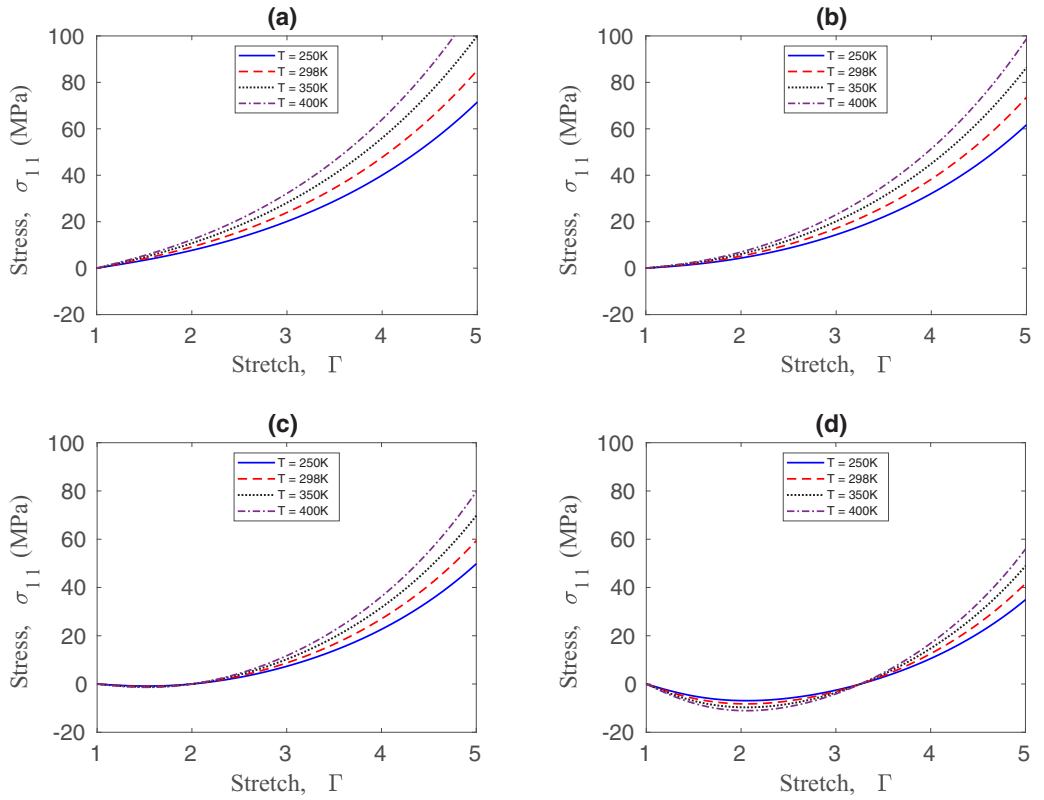

FIG. 10. Plots of σ_{11} with stretch Γ at varying temperatures, for crystallization ratios (a) $\Omega = 0$, (b) $\Omega = 0.15$, (c) $\Omega = 0.30$, (d) $\Omega = 0.45$.

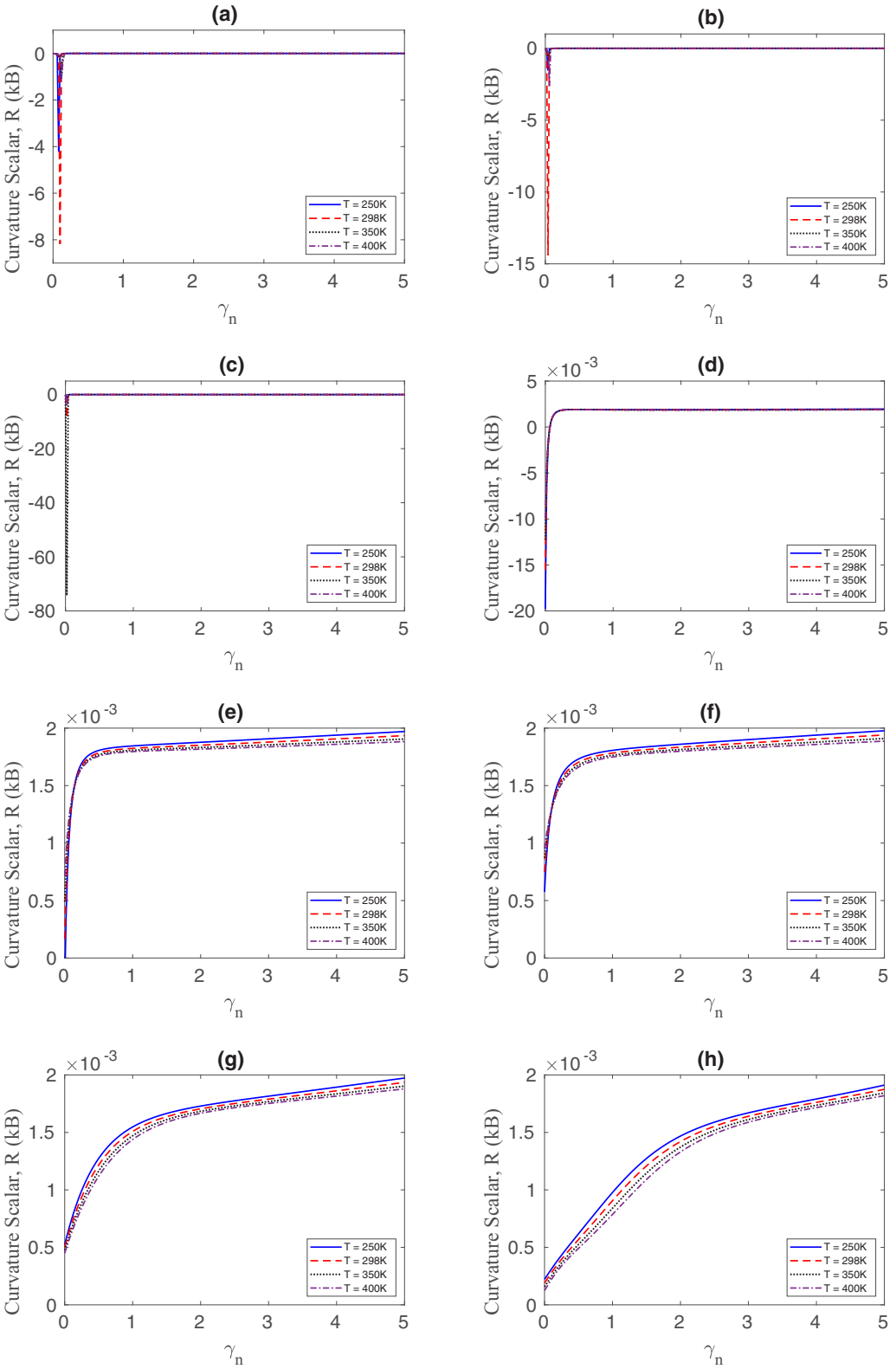

FIG. 11. Plots of scalar curvature R with stretch γ_n at varying temperatures, for crystallization ratios (a) $\Omega = 0$, (b) $\Omega = 0.15$, (c) $\Omega = 0.20$, (d) $\Omega = 0.30$, (e) $\Omega = 0.40$, (f) $\Omega = 0.45$, (g) $\Omega = 0.60$, (h) $\Omega = 0.70$.

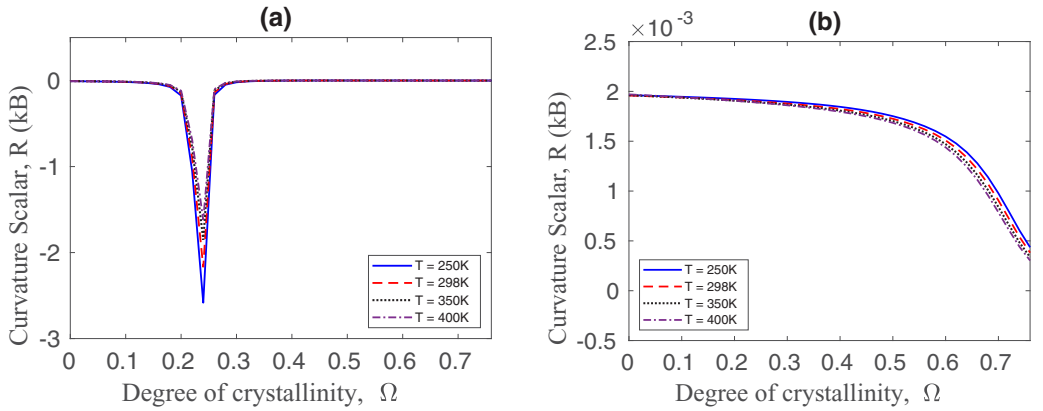

FIG. 12. Plots of scalar curvature R with degree of crystallinity Ω at varying temperatures, for (a) $\gamma_n = 0$, (b) $\gamma_n = 1$.

strain up to which the curvature remains nonzero is dependent on Ω and increases with it. From the plot corresponding to $\gamma_n = 0$ in Fig. 12 we obtain a negative peak at $\Omega = 0.23$. Peaks are observed at this location irrespective of the temperature. Recall that, in isochoric cases, we had obtained peaks at the same Ω value in plots of scalar curvature vs Ω for $\gamma = 0$ and $\Gamma = 1$ in Figs. 3 and 7 respectively. We had inferred that when $\Omega < \frac{1}{\sqrt{N}}$, the critical values of the strain and stretch should be $\gamma_{\rm cr} = 0$ and $\Gamma_{\rm cr} = 1$ respectively. Invoking the same rationale, we can conclude that the critical value of strain in this case must be 0, i.e., $\gamma_{ncr} = 0$.

But, we cannot identify the critical strain for $\Omega > \frac{1}{\sqrt{N}}$ from the curvature plots in Figs. 11 and 12 alone. In order to remove the spurious energy that evidently is present, as indicated by the nonzero curvature and strain energy at zero strain (See Figs. 11 and 14), we must resort to other conditions such as those derived from the mathematical expression of $\Psi_{\rm strain}$. Such conditions cannot be derived graphically.

Upon examination of the expressions of $\Psi_{\rm strain}$, $\Psi_{\rm vol}$, and $\Psi_{\rm dev}$, it is evident that the spurious energy is of the same form as $\Psi_{\rm dev}$, as $\Psi_{\rm vol}$ is identically zero. The condition under which $\Psi_{\rm dev} = 0$ is same as that stated in Eq. (26). Thus, for the nonisochoric case as well, we may assume that Eq. (26) defines the bounds on the spurious energy. Any pair of (γ_n, Ω) which satisfies condition Eq. (26) may thus be regarded as $(\gamma_{ncr}, \Omega_{\rm cr})$.

It should be noted that the uniaxial stress σ_{11} shown in Fig. 15 does not impart any significant information on the bounds. This is probably due to the dominating contribution of the volumetric component of stress.

In both isochoric and nonisochoric deformation for a chosen Ω, there exists a $\gamma_{\rm cr}$ or a $\Gamma_{\rm cr}$ or a γ_{ncr}, such that strain in excess of the critical value only contributes to the conformational isochoric strain energy. Having clarified the physical significance of these critical states, we must focus on how the spurious energy must functionally depend on the strain measure involving $\gamma_{\rm cr}$, $\Gamma_{\rm cr}$, or γ_{ncr}. As already emphasized, this energy is conformational and must be purely of the form $\Psi_{\rm dev}$ to effect a nonzero strain energy at zero strains.

V. MODIFIED FREE ENERGY

For both isochoric and nonisochoric cases, based on the arguments in the preceding sections, any strain leading to $\lambda_a < \lambda_{acr}$ contributes to the spurious energy, where λ_{acr} satis-

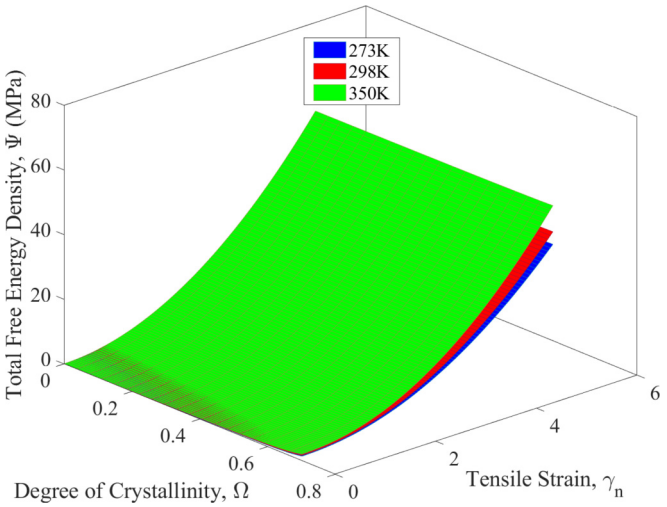

FIG. 13. Free energy surfaces for different temperatures T for nonisochoric deformation.

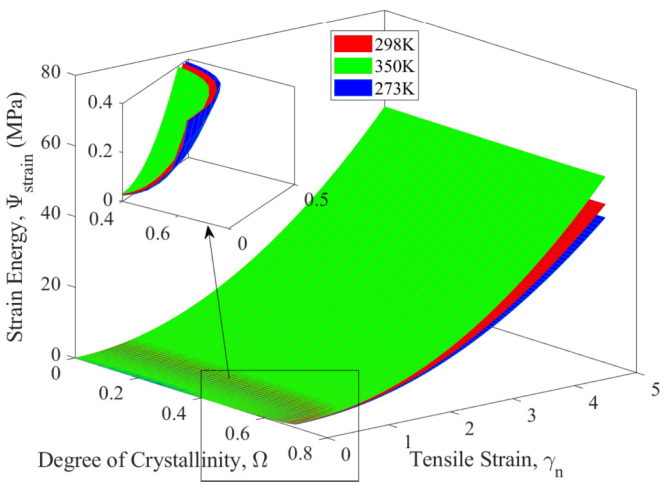

FIG. 14. Strain energy surfaces for different temperatures T for nonisochoric deformation.

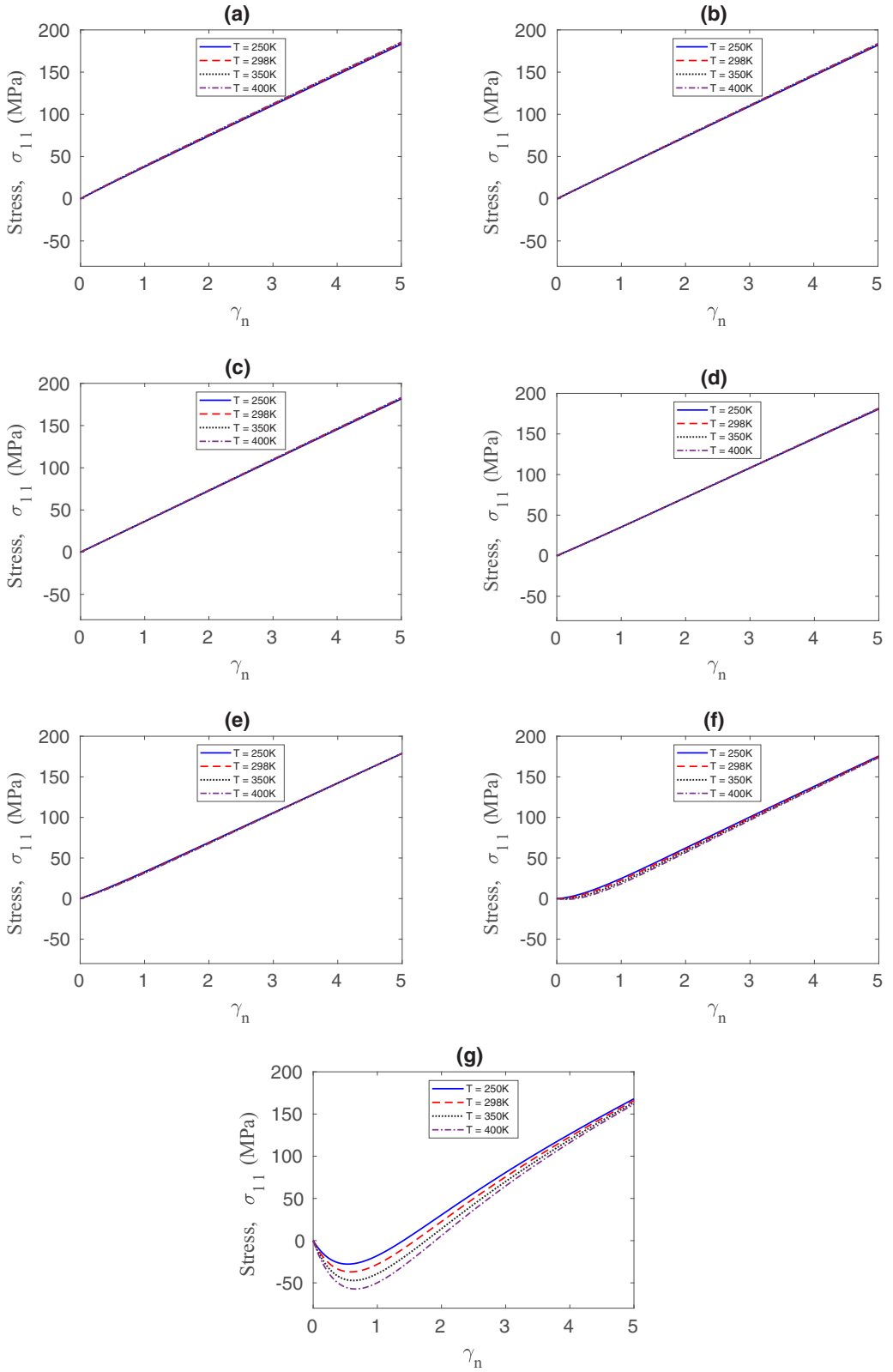

FIG. 15. Plots of σ_{11} with stretch γ_n at varying temperatures, for crystallization ratios (a) $\Omega = 0$, (b) $\Omega = 0.15$, (c) $\Omega = 0.20$, (d) $\Omega = 0.30$, (e) $\Omega = 0.45$, (f) $\Omega = 0.60$, (g) $\Omega = 0.70$.

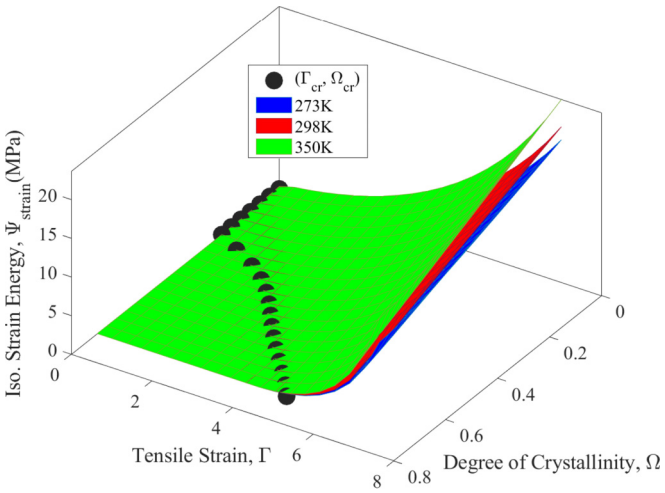

FIG. 16. Strain energy for isochoric uniaxial tension after removal of spurious component.

fies the following condition:

$$(\Omega\sqrt{N}-\lambda_{acr})H\left(\Omega-\frac{1}{\sqrt{N}}\right)+(1-\lambda_{acr})H\left(\frac{1}{\sqrt{N}}-\Omega\right)=0. \tag{29}$$

The spurious energy, which is the isochoric contribution due to $\lambda_a < \lambda_{acr}$, accordingly takes the form

$$\Psi_{\text{spur}} = k_B T N n(1-\Omega)H(\lambda_{acr}-\lambda_a) \times \left(\frac{3}{2}\Lambda_a^2+\frac{9}{20}\Lambda_a^4+\frac{99}{350}\Lambda_a^6\right). \tag{30}$$

The final free energy density is thus given by

$$\Psi = \Psi_{\text{vol}} + \Psi_{\text{dev}} - \Psi_{\text{spur}} + \Psi_{\text{cr}} + \Psi_{\text{surr}}. \tag{31}$$

The strain energy plots in Figs. 16 and 17 depict the corrected strain energy variation, where the spurious energy has been removed. This free energy may now be used to construct a constitutive theory for strain-induced crystallization in elastomers where stresses due to unphysical conformational energy are absent. Also, the energy driving the crystallization will not lead to an exaggerated crystallization ratio. In previous theories for strain induced crystallization such as [23], no such physical and systematic approach has been used to eliminate these unphysical components. The fundamental equations in these theories do not include any provisions for correcting the quantities, thus rendering the constitutive theories incomplete.

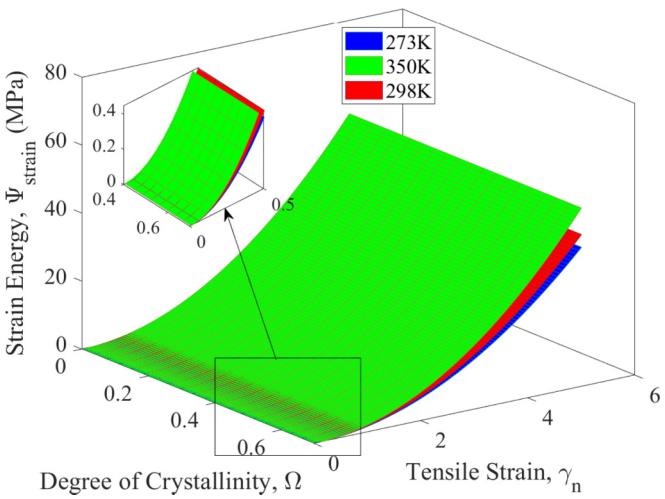

FIG. 17. Strain energy for uniaxial tension of a compressible solid after removal of spurious component.

VI. CONCLUSION

The classical fluctuation theory reveals significant information on underlying chain conformations in equilibrated polymers undergoing elastic deformation. However, in the case of inelastic deformation where relaxation occurs slowly enough for the hypothesis of local equilibrium to hold, the fluctuation theory may be still used to extract microstructural information regarding the thermodynamic system. One such piece of information would be regarding the proliferation and transformation of defects or incompatibilities responsible for the nonequilibrium response of the system. Additionally, if the fluctuation theory in consideration should be geometrically consistent in the sense of [3], an additional quantity is at our disposal: the Ricci curvature.

In this article we have tried to apply such a fluctuation theory to a thermodynamic system describing strain-induced-crystallization in elastomers. Instead of the fluctuation theorem, we are interested in the Riemannian curvature and the information it has to offer. For this thermodynamic system, the curvature imparts vital information on a spurious, crystallization-induced strain that results in a spurious isochoric energy. In the absence of a suitable correction, this energy leads to an unphysical stress and an erroneous evolution of crystallization. We determine this spurious strain from the curvature plots for both isochoric and nonisochoric strain states, though in the case of nonisochoric strains the graphically obtained information is not complete. We establish their unphysicality through an examination of the free energy and strain energy landscapes. Using this strain, we construct a modified free energy. It is evident from our study that the curvature does prove to be a vital quantity containing essential information on the physical viability of the thermodynamic states across the thermodynamic space even in nonequilibrium processes. In the case of crystallization, the curvature points to states with unphysical stretch components attributable to the geometric inconsistency while defining the stretch measures, which contributes to spurious strain energies. Thus the curvature yields constraints, extraneous to the constitutive relations of the thermodynamic forces and the evolution equations of internal variables and temperature. These constraints then need to be satisfied along with the balance laws plus the constitutive laws. The utility of curvature however is applicable to nonequilibrium processes where local equilibrium hypothesis can be applied.

The large deviation principle could be a possible approach to bypass the local equilibrium hypothesis and deal with nonequilibrium (steady-state, non-Gaussian) fluctuations in solids far from equilibrium. In such a case, it would

be crucial to appropriately represent the large deviation rate function and perhaps interpret it as a nonequilibrium counterpart of the free energy in some sense. However, a rational basis for this interpretation should be based on the "deterministic limit" for the generator of a Markov process of the jump-diffusion type [33]. This might also offer a probabilistic basis for coarse graining from meso- to macroscale. Such an approach, in the context of nonequilibrium thermodynamics of macroscopic solid continua, is worth investigation.

In addition to approaches involving the large deviation principle, our future efforts would include the study of curvature in other nonequilibrium phenomena. Specifically, we would like to study the implications of such a geometrically motivated fluctuation theory for glassy polymers undergoing viscoplastic deformation.

[1] G. Ruppeiner, Thermodynamic curvature measures interactions, Am. J. Phys. **78**, 1170 (2010).

[2] G. Ruppeiner, Riemannian geometry in thermodynamic fluctuation theory, Rev. Mod. Phys. **67**, 605 (1995).

[3] G. Ruppeiner, Thermodynamics: A Riemannian geometric model, Phys. Rev. A **20**, 1608 (1979).

[4] G. Ruppeiner and S. Bellucci, Thermodynamic curvature for a two-parameter spin model with frustration, Phys. Rev. E **91**, 012116 (2015).

[5] H.-O. May, P. Mausbach, and G. Ruppeiner, Thermodynamic curvature for attractive and repulsive intermolecular forces, Phys. Rev. E **88**, 032123 (2013).

[6] G. Ruppeiner, Thermodynamic curvature and phase transitions in Kerr-Newman black holes, Phys. Rev. D **78**, 024016 (2008).

[7] G. Ruppeiner, P. Mausbach, and H.-O. May, Thermodynamic geometry of the Gaussian core model fluid, Fluid Phase Equilib. **542**, 113033 (2021).

[8] G. Ruppeiner and A. Seftas, Thermodynamic curvature of the binary van der Waals fluid, Entropy **22**, 1208 (2020).

[9] X. Bu and X. Zhang, Scattering and gaussian fluctuation theory for semiflexible polymers, Polymers **8**, 301 (2016).

[10] E. M. Arruda and M. C. Boyce, A three-dimensional constitutive model for the large stretch behavior of rubber elastic materials, J. Mech. Phys. Solids **41**, 389 (1993).

[11] M. Tosaka, D. Kawakami, K. Senoo, S. Kohjiya, Y. Ikeda, S. Toki, and B. Hsiao, Crystallization and stress relaxation in highly stretched samples of natural rubber and its synthetic analogue, Macromolecules **39**, 5100 (2006).

[12] M. Tosaka, K. Senoo, S. Kohjiya, and Y. Ikeda, Crystallization of stretched network chains in cross-linked natural rubber, J. Appl. Phys. **101**, 084909 (2007).

[13] K. Brüning, K. Schneider, S. V. Roth, and G. Heinrich, Kinetics of strain-induced crystallization in natural rubber: A diffusion-controlled rate law, Polymer **72**, 52 (2015).

[14] B. Huneau, Strain-induced crystallization of natural rubber: a review of x-ray diffraction investigations, Rubber Chem. Technol. **84**, 425 (2011).

[15] E. B. Tadmor, R. E. Miller, and R. S. Elliott, *Continuum Mechanics and Thermodynamics: From Fundamental Concepts to Governing Equations* (Cambridge University Press, Cambridge, 2012)

[16] A. N. Beris and B. J. Edwards, *Thermodynamics of Flowing Systems: With Internal Microstructure*, Oxford Engineering Science Series Vol. 36 (Oxford University Press, Oxford, 1994)

[17] H. C. Öttinger, *Beyond Equilibrium Thermodynamics* (John Wiley & Sons, New York, 2005).

[18] D. J Evans and G. P Morriss, *Statistical Mechanics of Nonequilbrium Liquids* (ANU Press, Canberra, 2007).

[19] P. J. Flory, Thermodynamics of crystallization in high polymers. I. Crystallization induced by stretching, J. Chem. Phys. **15**, 397 (1947).

[20] M. Kroon, A constitutive model for strain-crystallising rubber-like materials, Mech. Mater. **42**, 873 (2010).

[21] J. Guilié, Comportement à la rupture et caractérisation mécanique des caoutchoucs cristallisants sous contrainte, Doctoral dissertation, Ecole Polytechnique X 2014, https://pastel.archives-ouvertes.fr/pastel-00978212.

[22] J. Guilié, T.-N. Le, and P. Le Tallec, Micro-sphere model for strain-induced crystallisation and three-dimensional applications, J. Mech. Phys. Solids **81**, 58 (2015).

[23] R. Rastak and C. Linder, A non-affine micro-macro approach to strain-crystallizing rubber-like materials, J. Mech. Phys. Solids **111**, 67 (2018).

[24] S. J. Mistry and S. Govindjee, A micro-mechanically based continuum model for strain-induced crystallization in natural rubber, Int. J. Solids Struct. **51**, 530 (2014).

[25] H. B. Callen, *Thermodynamics and an Introduction to Thermostatistics* (John Wiley & Sons, New York, 1998).

[26] I. M. Ward and J. Sweeney, *Mechanical properties of solid polymers* (John Wiley & Sons, New York, 2012).

[27] P. J. Flory, *Principles of Polymer Chemistry* (Cornell University Press, Ithaca, NY, 1953).

[28] L. Anand, A constitutive model for compressible elastomeric solids, Comput. Mech. **18**, 339 (1996).

[29] Q. Guo, F. Zaïri, and X. Guo, A thermo-viscoelastic-damage constitutive model for cyclically loaded rubbers. Part I: Model formulation and numerical examples, Int. J. Plast. **101**, 106 (2018).

[30] P. Chadwick, Thermo-mechanics of rubberlike materials, Philos. Trans. R. Soc. A **276**, 371 (1974).

[31] S. Kobayashi and K. Müllen, *Encyclopedia of Polymeric Nanomaterials* (Springer, Berlin, 2015).

[32] S. Wolfram, *Mathematica 8*, A system for doing mathematics by computer (Wolfram, Champaign, IL, 2010).

[33] L. Hong and H. Qian, Stochastic dynamics, large deviation principle, and nonequilibrium thermodynamics, Phys. Rev. E **104**, 044113 (2021).